Acta Biomaterialia 8 (2012) 4233–4243

Contents lists available at SciVerse ScienceDirect

Acta Biomaterialia

journal homepage: www.elsevier.com/locate/actabiomat

Biodegradable nanocomposite hydrogel structures with enhanced mechanical properties prepared by photo-crosslinking solutions of poly(trimethylene carbonate)–poly(ethylene glycol)–poly(trimethylene carbonate) macromonomers and nanoclay particles ☆

Shahriar Sharifi [a], Sebastien B.G. Blanquer [b], Theo G. van Kooten [a], Dirk W. Grijpma [a,b,*]

[a] W.J. Kolff Institute, Department of Biomedical Engineering, University Medical Centre Groningen, University of Groningen, P.O. Box 196, 9700 AD Groningen, The Netherlands
[b] MIRA Institute for Biomedical Technology and Technical Medicine, Department of Biomaterials Science and Technology, University of Twente, P.O. Box 217, 7500 AE Enschede, The Netherlands

ARTICLE INFO

Article history:
Available online 17 September 2012

Keywords:
Nanocomposites
Biodegradable hydrogels
PTMC–PEG–PTMC macromonomers
Photo-crosslinking
Stereolithography

ABSTRACT

Soft hydrogels with elasticity modulus values lower than 100 kPa that are tough and biodegradable are of great interest in medicine and in tissue engineering applications. We have developed a series of soft hydrogel structures from different methacrylate-functionalized triblock copolymers of poly(ethylene glycol) (PEG) with poly(trimethylene carbonate) (PTMC) by photo-crosslinking aqueous solutions of the macromonomers in 2.5 and 5 wt.% colloidal dispersions of clay nanoparticles (Laponite XLG). The length of the PTMC blocks of the macromonomers and the clay content determined the physicomechanical properties of the obtained hydrogels. While an increase in the PTMC block length in the macromonomers from 0.2 to 5 kg/mol resulted in a decrease in the gel content, the addition of 5 wt.% Laponite nanoclay to the crosslinking solution lead to very high gel contents of the hydrogels of more than 95%. The effect of PTMC block length on the mechanical properties of the hydrogels was not as pronounced, and soft gels with a compressive modulus of less than 15 kPa and toughness values of 25 kJ m^{-3} were obtained. However, the addition of 5 wt.% Laponite nanoclay to the formulations considerably increased the compressive modulus and resilience of the hydrogels; swollen nanocomposite networks with compressive modulus and toughness values of up to 67 kPa and 200 kJ m^{-3}, respectively, could then be obtained. The prepared hydrogels were shown to be enzymatically degradable by cholesterol esterase and by the action of macrophages. With an increase in PTMC block length in the hydrogels, the rates of mass loss increased, while the incorporated Laponite nanoclay suppressed degradation. Nanocomposite hydrogel structures with a designed gyroid pore network architecture were prepared by stereolithography. Furthermore, in the swollen state the porous gyroid structures were mechanically stable and the pore network remained fully open and interconnected.

1. Introduction

Hydrogels are hydrophilic networks that can take up very large amounts of water. Their biocompatibility and their consistency (which resembles the extracellular matrix (ECM)) make these materials very interesting for numerous applications in medicine and biomedical engineering [1]. In particular, biodegradable hydrogels are interesting materials from which to prepare matrices for cell encapsulation or scaffolding structures that support the adhesion and proliferation of cells. It has been demonstrated that variations in the rigidity of these highly compliant hydrogels can be a determining factor in regulating the cellular processes that determine the morphology, motility and differentiation of (mesenchymal stem) cells [2,3].

Despite their many advantageous properties, the brittleness and fragility of hydrogels has limited their use in load-bearing applications such as in the regeneration of cartilage, tendon, dermis and arterial walls [4]. While many natural hydrogel structures combine a high uptake of body fluids with low elasticity modulus, high elongation at break and high toughness, most synthetic hydrogels that are currently used in medical applications and tissue engineering easily fracture under only mild loading conditions.

☆ Part of the Special Issue "Advanced Functional Polymers in Medicine (AFPM)", guest editors: Professors Luigi Ambrosio, Dirk W. Grijpma and Andreas Lendlein.

* Corresponding author at: MIRA Institute for Biomedical Technology and Technical Medicine, Department of Biomaterials Science and Technology, University of Twente, P.O. Box 217, 7500 AE Enschede, The Netherlands. Tel.: +31 534892966.
E-mail addresses: d.w.grijpma@utwente.nl, d.w.grijpma@umcg.nl (D.W. Grijpm).

1742-7061/$ - see front matter © 2012 Acta Materialia Inc. Published by Elsevier Ltd. All rights reserved.
http://dx.doi.org/10.1016/j.actbio.2012.09.014

Recently novel synthetic hydrogel systems have been developed that show excellent toughness and resilience. These systems include polyrotaxane-based hydrogels [5], nanocomposite hydrogels [6] and double-network hydrogels [7]. Nevertheless, the development of biodegradable synthetic hydrogels with mechanical and biological features similar to those of natural hydrogels remains a challenge.

The preparation of network structures with colloidally dispersed nanosized fillers has been an effective approach to increase the elastic modulus, strength and toughness of hydrogels. Layered silicate nanoparticles or nanoplatelets such as Laponite have been of special interest, as they are hydrophilic and can easily be dispersed and exfoliated in aqueous media [8]. Furthermore, recent studies have shown the compatibility of these clays with a variety of cell types [9,10] and much research has been conducted on the preparation and properties of nanocomposite hydrogels with Laponite for biomedical applications [8–13].

Chang et al. [11] reported that incorporation of 8 wt.% Laponite nanoparticles into polyethylene glycol (PEG) diacrylate hydrogels significantly enhanced the compressive and tensile properties of the hydrogels. Tough elastomeric hydrogels with high elongations at break in tensile tests were obtained. Similarly, Wu et al. [14] showed that Pluronic F127 diacrylate hydrogels reinforced with nanoclay particles can have a low elasticity modulus of 10 kPa while at same time are tough rubber-like materials with very high elongations at break. Gaharwar et al. [12] reported physically cross-linked poly(ethylene oxide) (PEO) hydrogels using up to 3.5 wt.% Laponite nanoclay. In these PEG hydrogels, the surface of the Laponite nanoclay provides an interface on which PEG chains can physically adsorb, thereby leading to formation of a junction between different PEG chains and finally formation of a Laponite–PEG network. This is especially the case when the molecular weight of the PEG component is relatively high (higher than ~13 kg mol^{-1}) [11].

There has been great interest in soft and tough biodegradable hydrogels. As PEG-acrylate or PEG-methacrylate networks are not biodegradable, Varghese and co-workers prepared crosslinked triblock copolymers of PEG and poly(trimethylene carbonate) (PTMC–PEG–PTMC) networks that combine biodegradability with good toughness. By adjusting the ratio of hydrophilic PEG to hydrophobic PTMC segments, hydrogels with low elastic modulus values of 15 kPa and high toughness were obtained. The hydrogels were hydrolytically and enzymatically degradable, and also supported the adhesion of mesenchymal stem cells and bovine chondrocytes [15,16].

In this work, we investigated the effect of the incorporation of clay nanoparticles on the mechanical and biological properties of photo-crosslinked PTMC–PEG–PTMC hydrogels. By photo-crosslinking aqueous micellar dispersions/solutions of the corresponding macromonomers in the nanoclay dispersions, we obtained biodegradable hydrogels in which the crosslinks are formed by physical interaction of the PEG segments with the nanoclay and covalent ones through polymerization of the functional end-groups. The hydrophobic PTMC-block length was systematically varied to assess its effect on the physical properties of the macromonomer dispersions/solutions and the resulting hydrogels after crosslinking. The enzymatic degradation behavior and the effect of macrophages was investigated. It is also shown that designed structures can be built from these materials by stereolithography.

2. Materials and methods

2.1. Materials

PEG (M_n = 20 kg mol^{-1}), stannous octoate (tin(II) 2-ethylhexanoate), triethylamine (TEA), methacrylic anhydride (MAA), hydroquinone and anhydrous dichloromethane (DCM) were purchased from Sigma-Aldrich, The Netherlands. Trimethylene carbonate (TMC) was purchased from Boehringer Ingelheim, Germany, n-hexane from Acros Organics, Belgium. Irgacure 2959 (2-hydroxy-1-[4-(2-hydroxyethoxy)phenyl]-2-methyl-1-propanone) and Orasol Orange G, an orange dye soluble in organic solvents, were obtained from Ciba Specialty Chemicals, Switzerland.

Laponite XLG nanoparticles ($Na^{+}_{0.7}[(Mg_{5.5}Li_{0.3})Si_8O_{20}(OH)_4]^{-}_{0.7}$, with average diameter of 30 nm and thickness of 1 nm and a cationic exchange capacity of 50–60 meq/100 g) was a gift from Rockwood Additives, USA. The deionized water used was purified with a Milli-Q system (Millipore, USA), phosphate-buffered saline (PBS, pH 7.4) was obtained from Biochrom (Germany). DMEM (Dulbecco's Modified Eagle's Medium) with 4.4 g l^{-1} D-glucose supplemented with penicillin (100 units ml^{-1}), streptomycin (100 μg ml^{-1}), GlutaMAX™-I (200 mM in 0.85% NaCl, 100 times diluted) and fetal bovine serum (FBS) were obtained from Invitrogen (Gibco, USA). Trypsin-EDTA (0.05%), DAPI (4,6-diamidino-2-phenylindole), TRITC-phalloidin and bovine serum albumin were purchased from Invitrogen, The Netherlands. Triton X-100 was purchased from Sigma-Aldrich and diluted to 0.05% in PBS. ATCC cell lines, J774A mouse macrophage (ATCC-TIB-67), were obtained from the American Type Culture Collection. Cholesterol esterase (CE) from porcine pancreas, piperazine-1,4-bis(2-ethanesulfonic acid) (PIPES) and ethylene glycol tetraacetic acid (EGTA) were obtained from Sigma-Aldrich, the Netherlands. Lucirin TPO-L (ethyl 2,4,6-trimethylbenzoylphenyl phosphinate) was obtained from BASF (Germany). All chemicals were reagent grade and used as received unless mentioned otherwise.

2.2. Synthesis of PTMC–PEG–PTMC triblock macromonomers

PTMC–PEG–PTMC triblock copolymers with different PTMC block lengths were prepared by ring-opening polymerization of TMC initiated by PEG. In a typical reaction, 1 g of TMC (10 mmol) and 50 g of PEG 20 kg mol^{-1} (2.5 mmol, dried by azeotropic distillation in toluene) were mixed and stannous octoate (2×10^{-4} mol mol^{-1} TMC) was added. The mixture was polymerized under an inert argon atmosphere at 130 °C for 72 h. The triblock copolymers were then functionalized with methacrylate end-groups by reaction with MAA in the presence of TEA as reported elsewhere [17] and purified by precipitation in diethyl ether and subsequent drying in a vacuum oven at 45 °C. PTMC–PEG–PTMC macromonomers with PTMC block lengths of 0, 0.2, 0.5, 1 and 5 kg mol^{-1} were prepared. The synthesized oligomers and corresponding macromonomers are respectively referred to as $PTMC_y$–PEG–$PTMC_y$ and MA–$PTMC_y$–PEG–$PTMC_y$–MA, where y denotes the PTMC block length in kg mol^{-1}.

2.3. Preparation of PTMC–PEG–PTMC nanoclay composite hydrogels

PTMC–PEG–PTMC hydrogels and composite hydrogels with Laponite nanoclay were prepared by photo-polymerization of aqueous solutions of MA–PTMC–PEG–PTMC–MA macromonomers and the Laponite nanoclay using hydrophilic Irgacure 2959 as initiator. First homogeneous colloidal dispersions of (exfoliated) Laponite XLG in deionized water were prepared while stirring vigorously, then the different MA–PTMC–PEG–PTMC–MA macromonomers and photo-initiator were dissolved into the nanoclay dispersion.

Different photo-crosslinkable formulations containing Laponite nanoclay concentrations of 2.5 and 5 wt.% were prepared. In all formulations, the macromonomer concentration was 12.5 wt.%, while the Irgacure 2959 concentration was 2 wt.% with respect to the macromonomer.

Photo-crosslinking was then conducted in 24-well tissue culture polystyrene (TCPS) cell culture plates (Nalgene, Germany). 2 ml portions of the various macromonomer–Laponite nanoclay solutions were added to the wells of the culture plate. Centrifugation at room

temperature for 10 min at 2500 rpm using a plate centrifuge apparatus (Eppendorf 5810R, Germany) ensured that air bubbles were removed. Centrifugation did not have any effect on the homogeneity of the colloidal dispersions and solutions. The solutions were then photo-crosslinked in a crosslinking cabinet (Ultralum, USA) under a constant nitrogen flow for 800 s using a 365 nm UV lamp at 10 cm from the surface of the specimens. Neat PTMC–PEG–PTMC hydrogels were prepared by the same procedure used for the nanocomposite hydrogels, except that no Laponite nanoclay was added to the formulations.

The prepared networks are referred to as NC_xTMC_y. Here x denotes the concentration (wt.%) of Laponite XLG nanoclay in the precursor solution that was photo-crosslinked, and *y* denotes the length of PTMC block in kg mol^{-1} in the MA–PTMC–PEG–PTMC–MA macromonomer that was used. For example: $NC_5PTMC_{0.5}$ refers to a crosslinked hydrogel that was prepared by photo-crosslinking solution containing 5 wt.% Laponite nanoclay and 12.5 wt.% MA–$PTMC_{0.5}$–PEG–$PTMC_{0.5}$–MA macromonomer. Formulations prepared from the macromonomers with the highest TMC contents (MA–$PTMC_5$–PEG–$PTMC_5$–MA) containing 2.5 and 5 wt.% clay were too viscous to allow homogeneous mixing, and therefore $NC_{2.5}$ $PTMC_5$ and NC_5PTMC_5 networks were not prepared.

2.4. Characterization of synthesized oligomers, macromonomers, hydrogels and networks

Proton nuclear magnetic resonance (^{1}H-NMR) using deuterated DMSO as solvent was used to quantify the number of –OH groups in the PEG initiator and to determine its molar mass. Spectra were recorded at ambient temperature using a 300 MHz spectrometer (Varian Inova, USA).

Using $CDCl_3$ as the solvent, the TMC monomer conversions in the PTMC–PEG–PTMC block copolymer synthesis were determined from the integral values of peaks corresponding to methylene units of the monomer (2.43 ppm) and of the oligomer (4.24 ppm). The average number of TMC units in the block copolymers was calculated from the relative integral values of the methylene protons of TMC units, –(C=O)–O–CH_2–CH_2–CH_2–O– at 2.1 ppm and of the methylene protons of the ethylene oxide repeating units in the PEG at 3.6 ppm. This then also allowed the calculation of the molar mass of the macromonomers.

The degrees of functionalization (DF) of the macromonomers were determined from the relative integral values of the methacrylate protons at 5.7 ppm and the methylene protons of the ethylene oxide repeating units at 3.6 ppm.

The thermal properties of the macromonomers were evaluated by differential scanning calorimetry (DSC) using a PerkinElmer Pyris DSC apparatus. Samples weighing 5–10 mg were heated to 100 °C at a rate of 10 °C min^{-1}, and then cooled to −50 °C at a rate of 5 °C min^{-1}. A second scan was then recorded from −50 to 100 °C at 10 °C min^{-1}. The glass transition temperature, T_g, of the specimens was determined as the midpoint of the change in the heat capacity.

Dynamic light scattering (DLS) measurements of solutions of the MA–PTMC–PEG–PTMC–MA macromonomers in water (0.25 and 0.5 g ml^{-1}) were conducted to determine aggregate or micellar sizes of the solutions. Experiments were carried out at room temperature using a Malvern Nano ZS (USA). The laser used had a wavelength of 633 nm, and the scattering angle was 173°.

The network characteristics of the photo-crosslinked specimens were assessed in swelling experiments at room temperature using DCM and PBS as swelling agents. The as-prepared hydrogels were first dried in a vacuum oven at 45 °C until they attained a constant weight, and their dried mass was determined (m_i). These samples were then immersed in excess DCM or PBS for 5 days, and their wet mass was determined (m_s) after blotting their surfaces. The specimens were then redried in a vacuum oven at 45 °C for 3 days and again their dry mass was determined (m_d). The equilibrium degree of swelling of the networks in DCM and PBS (Q) and their gel fractions in DCM were determined in triplicate using:

$$Q = 1 + \frac{m_s - m_d}{m_d} \times \frac{\rho_{\text{macromonomere}}}{\rho_{\text{DCM}} \text{ or PBS}} \quad (1)$$

$$\text{Gel fraction } (\%) = \frac{m_d}{m_i} \times 100. \quad (2)$$

The densities of the macromonomers, water and DCM used were respectively: $\rho_{\text{macromonomer}}$ = 1.20 g cm^{-3}, ρ_{DCM} = 1.33 g cm^{-3} and ρ_{PBS} = 1.00 g cm^{-3}.

2.5. Mechanical properties of PTMC–PEG–PTMC hydrogels and nanoclay hydrogel composites

The mechanical properties of hydrated PTMC–PEG–PTMC hydrogels and their Laponite nanoclay composite were determined in compression. The as-prepared, cylindrically shaped hydrogel specimens were swollen in PBS for approximately 7 days at room temperature to reach equilibrium. The specimens were then compressed at a rate of 10 mm min^{-1} using a Zwick Z020 tensile tester at room temperature (20 °C). From the compression stress–strain curves, values of compressive modulus (E_c), strain at break (ε_{break},) and stress at break (σ_{break}) were determined. The compressive modulus was calculated from the slope of the curves at strains between 5% and 20%.

2.6. Enzymatic degradation of PTMC–PEG–PTMC hydrogels and nanoclay hydrogel composites by cholesterol esterase

Porcine pancreatic CE was used to study the enzymatic degradation of the (composite) PTMC–PEG–PTMC hydrogels. CE enzyme solutions were prepared at a concentration of 20 μg ml^{-1} in PBS containing 0.1 wt.% NaN_3 (Sigma, USA) as a bactericide. As-prepared hydrogels were first swollen in PBS for 7 days to extract the water-soluble sol part of the network and then dried at 45 °C for 3 days. Cylindrical specimens (approximately 5 mm in diameter, 5 mm in height, n = 3 per time point) were placed in vials containing 5 ml of the enzyme solution in PBS at 37 °C for up to 5 weeks. The medium was refreshed every 2 days. At the end of this time point, the specimens were dried at 45 °C in a vacuum oven until constant weight. The loss of dry mass was used as an indication of the extent of degradation.

2.7. Culturing of macrophages on PTMC–PEG–PTMC hydrogels and nanoclay hydrogel composites

To assess the effect of the TMC component in the PTMC–PEG–PTMC hydrogels and of the Laponite nanoclay content in the hydrogel composites, cell culturing experiments on different PTMC–PEG–PTMC hydrogels were done using murine macrophages. Hydrogel specimens prepared from aqueous solutions of PEG-dimethacrylate and MA–$PTMC_1$–PEG–$PTMC_1$–MA containing 0, 2.5 and 5 wt.% Laponite nanoclay were selected for this.

The hydrogels were prepared as described in above and were extracted twice in PBS for approximately 48 h to leach out any unreacted macromonomer. The specimens were disinfected using aqueous solutions of ethanol in water with increasing ethanol concentrations (20–70% ethanol). The specimens were then carefully de-swollen with aqueous ethanol solutions of decreasing concentrations. The gels were then extracted with PBS and subsequently with DMEM medium for another 2 days. The solutions and media were replaced every 12–24 h.

The attachment and proliferation of macrophages on the hydrogels and their capability to degrade their surface was investigated

by culturing J774A macrophages on the hydrogels. J774A macrophages were maintained in DMEM containing 4.5 g l^{-1} D-glucose, pyruvate, 10% FBS, 100 U ml^{-1} penicillin, and 100 μg ml^{-1} 2 mM Glutamax™. Cells were passaged every 4–7 days by scraping. Cells were then seeded (390000 cells $well^{-1}$) and cultured on the surface of the hydrogels with refreshment of the medium every 3–4 days. After two time points, at 7 and 10 days, the samples were fixed with 3.7% paraformaldehyde in cytoskeletal stabilizing buffer for 15 min, and then transferred to PBS. Samples were then subjected to fluorescence staining of the nuclei using DAPI and of the actin cytoskeleton using TRITC–phalloidin. These specimens were then analyzed by confocal laser scanning microscopy (Leica TCS SP2, Germany with a fully water immersed 40× objective (NA 0.80)).

2.8. Stereolithographic preparation of designed PTMC–PEG–PTMC nanoclay composite hydrogel structures

Designed structures were made from a solution of MA–$PTMC_{0.5}$–PEG–$PTMC_{0.5}$–MA containing 2 wt.% Laponite nanoclay using a slightly modified version of a procedure that was reported previously [18]. In brief, the MA–$PTMC_{0.5}$–PEG–$PTMC_{0.5}$–MA macromonomer was dissolved in a propylene carbonate water mixture (80:20 v/v) containing 2 wt.% Laponite nanoclay to a final concentration of 15 wt.%. The Lucirin TPO-L photo-initiator and Orasol Orange D dye to control the penetration depth of the light were added at respective concentrations of 5 and 0.15 wt.% relative to the macromonomer. Cylindrical, three-dimensional porous structures with gyroid pore network architectures, an average pore size of 600 μm and a porosity of 70% were designed using K3dSurf v. 0.6.2 (http://www.k3dsurf.sourceforge.net) and Rhinoceros 3D (McNeel, Europe) software. These designs were then built at a pixel resolution of $16 \times 16\ \mu m^2$ and sequential layer thicknesses of 25 μm using the above-mentioned nanocomposite resin and a Perfactory Mini Multilens (EnvisionTec, Germany) stereolithography apparatus (SLA) as described by Seck et al. [18]. From the working curve that was determined for the resin, this required each layer to be illuminated for 42 s at an intensity of 20 mW cm^{-2}. After building, the structures were carefully extracted at room temperature several times with water over a period of 5 days. The mechanical properties of the prepared designed porous structures were determined in compression as previously described.

3. Results and discussion

3.1. Synthesis and characterization of PTMC–PEG–PTMC macromonomers

A series of PTMC–PEG–PTMC triblock copolymers with different molar ratios of PEG and PTMC were synthesized by initiating the ring-opening polymerization of TMC with the terminal hydroxyl groups of PEG. ^{1}H-NMR of the non-purified copolymers showed that the TMC monomer conversion was approximately 92%. The molecular structure of the prepared PTMC–PEG–PTMC triblock copolymers could also be characterized by ^{1}H-NMR. In the spectra, characteristic peaks of the PTMC and PEG blocks could be identified: from the PTMC block –(C═O–O–C**H$_2$**–CH_2–C**H$_2$**–O– protons at 4.2 ppm and –(C═O)–O–CH_2–C**H$_2$**–CH_2–O– protons at 2.1 ppm were present, from the PEG blocks –C**H$_2$**C**H$_2$**O– protons at 3.6 ppm were present. After functionalization with methacrylate anhydride, the distinctive signals of the double bond end-groups could be distinguished at 5.6 and 6.1 ppm. Table 1 gives an overview of the molecular weights, respective block lengths and chemical structures, and degrees of functionalization of the triblock copolymers that could be determined.

The results show that the molecular weights of PEG and of the synthesized oligomers and macromonomers corresponded very well with the expected or intended values. With increasing TMC content in the feed during the copolymerization reaction, the resulting length of the PTMC block increased. The reaction with methacrylic anhydride yielded macromonomers with high degrees of functionalization, 85–92%.

Table 1 also shows the thermal characteristics of the obtained triblock copolymer macromonomers in the non-hydrated state. It can be seen that all macromonomers are semicrystalline with a peak melting temperature close to 60 °C, which is characteristic for the PEG component. With increasing TMC content and block length, the melting point decreases somewhat. The glass transition temperature (T_g) of PTMC and PEG have been reported to be −15 °C [19] and −54 °C [20], respectively. The macromonomers show a single glass transition temperature varying between approximately −59 and −45 °C. The glass transition temperature increases with increasing TMC content. The increased molecular weight of the macromonomers can also contribute to higher T_g values.

3.2. Network properties of PTMC–PEG–PTMC hydrogels and nanoclay hydrogel composites

A series of PTMC–PEG–PTMC networks were prepared by photocrosslinking MA–PTMC–PEG–PTMC–MA macromonomers in aqueous solutions containing varying amounts of Laponite nanoclay.

Fig. 1A shows images of the macromonomer solutions in water, the as-prepared hydrogels and the PTMC–PEG–PTMC hydrogels swollen to equilibrium in PBS. Depending on the TMC content, transparent to opaque macromonomer solutions (and corresponding crosslinked hydrogels) were obtained. In aqueous media, the triblock copolymeric macromonomers can form micelles in which the hydrophobic PTMC segments and the methacrylate groups form the cores of the micelles and the hydrophilic PEG segments either loop back into the micelles or form a bridge to neighboring micelles [21]. These micellar structures are dynamic in nature, which implies that a transient network can be formed. With increasing PTMC block lengths, phase separation between the hydrophilic PEG blocks and the hydrophobic PTMC blocks will increase. In the aqueous environment, the hydrophobic PTMC components will associate into larger clusters and the viscosity of the micellar triblock copolymeric solution will increase [22,23].

Particle size measurements of the macromonomer solutions (dispersions) in water by DLS indeed showed that the size of the micelles or aggregates depended on the length of hydrophobic

Table 1
Characteristic properties of synthesized PTMC–PEG–PTMC macromonomers.

Macromonomer	Length of PTMC block (kg mol^{-1}, intended)	M_n, (kg mol^{-1}, NMR)	Length of PTMC block (g mol^{-1}, NMR)	DF (%)	T_g (°C)	T_m (°C)	Particle or aggregate size (nm)
MA–PEG–MA	0	20.1	0	85	−58.9	60.3	Soluble
MA–$PTMC_{0.2}$–PEG–$PTMC_{0.2}$–MA	0.2	20.3	113	90	−55.9	60.1	12.8 ± 0.1
MA–$PTMC_{0.5}$–PEG–$PTMC_{0.5}$–MA	0.5	20.8	364	92	−54.8	59.0	227.9 ± 7.5
MA–$PTMC_1$–PEG–$PTMC_1$–MA	1	21.8	840	90	−52.1	58.7	300.3 ± 36
MA–$PTMC_5$–PEG–$PTMC_5$–MA	5	29.3	4580	87	−45.3	58.4	1364 ± 12

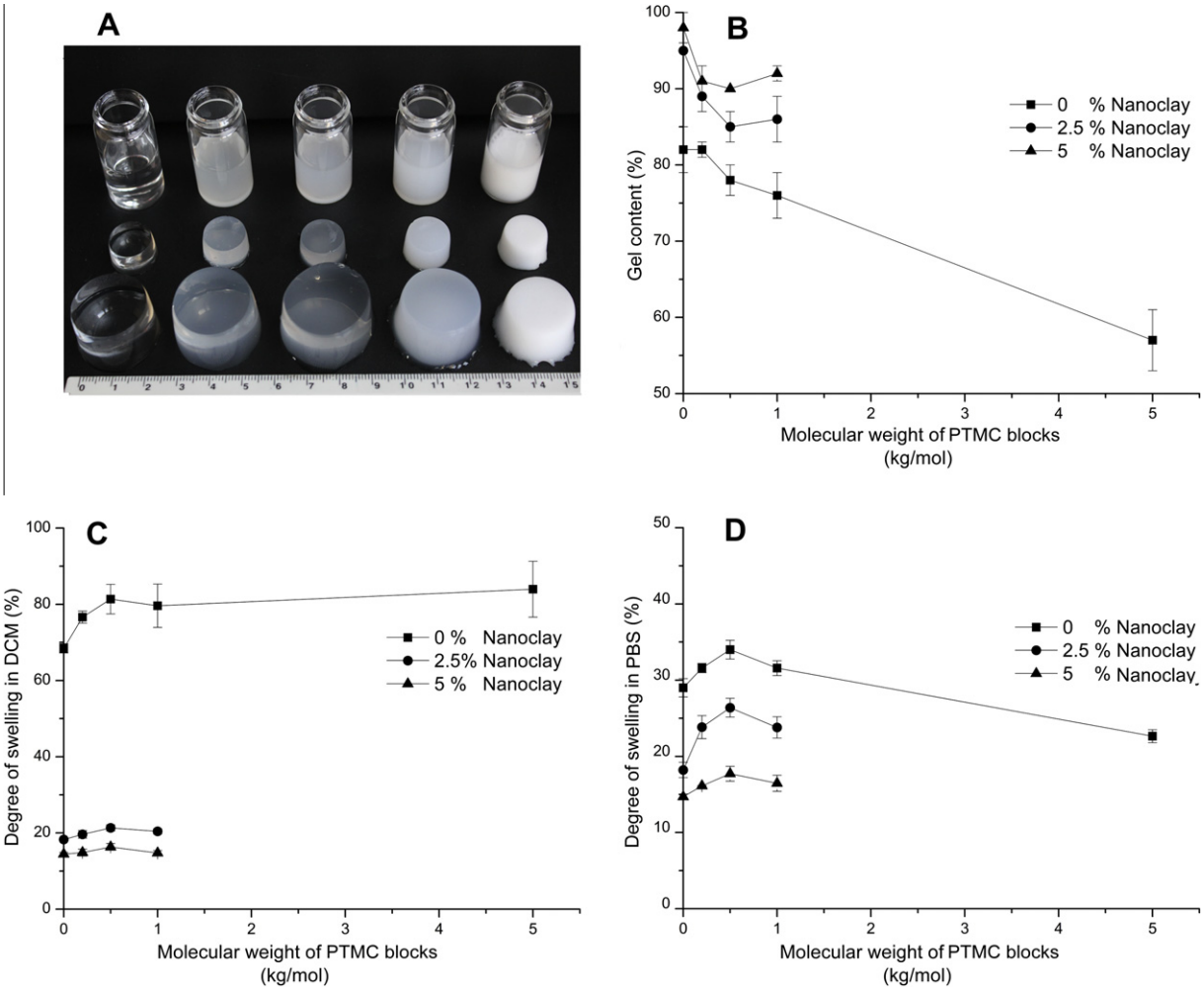

Fig. 1. Properties of hydrogels prepared by photo-crosslinking aqueous solutions of PTMC–PEG–PTMC macromonomers. (A) Appearance of the solutions to be crosslinked (top row), the as-prepared hydrogels (middle row) and the hydrogels equilibrated in water (bottom row). From left to right: NC_0PTMC_0, $NC_0PTMC_{0.2}$, $NC_0PTMC_{0.5}$, NC_0PTMC_1 and NC_0PTMC_5 hydrogels. The effect of the PTMC block length of the PTMC–PEG–PTMC macromonomers and the Laponite XLG nanoclay particle concentration in the crosslinking solution on: (B) the gel content of the obtained hydrogels; (C) the degree of swelling in dichloromethane; (D) the degree of swelling in PBS.

PTMC segments. Table 1 shows that with increasing hydrophobic block length, aggregate sizes in the micrometer range are obtained. The transparency of solutions decreases significantly with increasing TMC content. leading to the formation of opaque hydrogels after photo-crosslinking (Fig. 1A).

The prepared networks and nanoclay composite networks were characterized after drying by swelling experiments in DCM and PBS. While DCM is a good solvent for PEG as well as for PTMC, water and PBS are only good solvents for PEG and not for PTMC.

The gel content of hydrogels after extraction at room temperature with DCM is shown in Fig. 1B. The gel content of the prepared networks decreases with an increase in the PTMC block length of the macromers. In the micellar solutions, the aqueous phase contains the hydrophilic photo-initiator and the PEG blocks, while the PTMC blocks with the methacrylate end-groups form the hydrophobic cores of the micelles that are less accessible for the initiating radicals. Upon photo-crosslinking, the transient micellar network is fixed. Scheme 1 illustrates schematically the process of dissolving/dispersing the macromonomers in aqueous media and the preparation of nanocomposite hydrogel networks in the presence of exfoliated Laponite nanoplatelets.

Networks with the highest gel contents are prepared from macromer solutions with the highest clay nanoparticles contents and the lowest TMC amounts. In the absence of nanoparticles, this can be attributed to differences in solubility of the PTMC and PEG blocks in water, and therefore to differences in solubility of the macromers in the aqueous solutions that are crosslinked and have increased viscosities, and to differences in the molecular weights of the macromers. (Note that $NC_{2.5}PTMC_5$ and NC_5PTMC_5 networks were not prepared.)

In Fig. 1C the swelling ratios of the different networks in DCM are shown. A limited increase in the degrees of swelling with increasing TMC contents and block length is observed. This is the result of the formation of less densely crosslinked networks. Much more significant is the effect of the Laponite nanoclay in the composite networks. For all macromonomer compositions the addition of 2.5 or 5 wt.% Laponite nanoclay to the crosslinking solution not only greatly increased the gel contents of the formed nanocomposite networks (Fig. 1B), but also greatly decreased their degrees of swelling in DCM as shown in Fig. 1C, indicating the additional formation of physical crosslinks in the presence of the hydrophilic Laponite nanoclay platelets.

With regard to potential applications as degradable hydrogels, the behavior of the nanocomposite PTMC–PEG–PTMC networks in PBS is important. The swelling characteristics in PBS are shown in Fig. 1D. It is clear from the figure that while both network composition and Laponite nanoclay content have an important effect on the uptake of water, the swelling of the networks is less than in DCM.

When considering the effect of the TMC content in the macromonomers and networks on the swelling behavior in PBS, the uptake first increases with increasing block length of the PTMC units in the macromonomers used to prepare the networks and then decreases again (Fig. 1B). As the PTMC block lengths increase, the molecular weight between crosslinks in the networks increases. As the PTMC block length further increases, however, hydrophobicity of the network also increases, which limits the affinity for water. In a similar way, Zhang et al. varied the physicomechanical properties of neat PTMC–PEG–PTMC hydrogels by controlling the hydrophilic/hydrophobic balance of the macromonomers [15].

Despite the ionic and hydrophilic nature of the Laponite nanoclay particles, which can favor the uptake of water [24], the incorporation of nanoclay particles in the hydrogel network greatly reduced their swelling capacity in water. Since the degree of equilibrium swelling of a network is inversely proportional to its crosslink density [25], this implies that besides the covalent crosslinks formed during photo-polymerization of the macromonomers, additional physical crosslinks have been formed in the presence of the Laponite nanoclay. Physical interactions of nanoclay platelets with polymer chains have been reported before. It is known, for example, that PEO adsorbs on the surfaces of Laponite nanoclay platelets [26]. Chang et al. [11] showed that both low and high molecular weights PEG can form physical networks in the presence of these nanoclays.

3.3. Mechanical properties of PTMC–PEG–PTMC hydrogels and nanoclay hydrogel composites

The mechanical properties of equilibrium swollen PTMC–PEG–PTMC hydrogels and PTMC–PEG–PTMC nanocomposite hydrogels with Laponite nanoclay were assessed in unconfined compression tests. An overview of the mechanical characteristics is presented in Fig. 2.

As can be seen in Fig. 2A, the molecular weight of the hydrophobic PTMC block has an important effect on the elastic modulus of the resulting hydrogels. Although it could be expected that an increase in the PTMC segment length, which leads to an increased hydrophobicity, would lead to higher values of the elasticity modulus of the swollen hydrogels, the figure shows that the trend is the opposite. As the length of the hydrophobic PTMC block was increased from 0 to 5 kg mol^{-1}, the compression modulus of the hydrogels that did not contain nanoclay particles decreased by more than a factor of 2 from 15 to 6.7 kPa. The crosslinkable methacrylate groups that upon crosslinking will account for the mechanical behavior of the hydrogels are located in the micellar cores [15,27]. Due to changes in the solubility of the macromonomers in water as shown before, increasing the PTMC segment length results in lower crosslink densities of the hydrogels and therefore in lower compressive modulus values.

The PTMC block length also influenced the maximum compressive strength and toughness (determined from the area under the compression stress–strain diagram) of the PBS-swollen PTMC–PEG–PTMC hydrogels as shown in Fig. 2B and C. This effect was most pronounced for the NC_0PTMC_0, $NC_0PTMC_{0.2}$ and $NC_0PTMC_{0.5}$ hydrogels. Despite a decrease in the elastic modulus, the compressive strength and toughness of these hydrogels increased when the PTMC block length increased from 0 to 0.5 kg mol^{-1}. This suggests that in this region the increased TMC content enables the hydrogels to withstand higher stresses due to the synergistic effect of the dissipation of energy from random coil formation of PTMC chains and the controlled water absorption in the hydrogels [15]. The compressive strains at break values for these gels were a minimum of 75% (NC_0PTMC_0 gels) and a maximum of 87% for the $NC_0TMC_{0.5}$ hydrogels.

All PTMC-containing hydrogels were soft gels in the swollen state and showed rubber-like behavior; after compression to strains below their breaking strains they completely recovered to their initial dimensions. For these hydrogels it was observed that increasing their PTMC content did not necessarily result in enhanced mechanical properties. Surprisingly, NC_0PTMC_1 and NC_0PTMC_5 hydrogels had similar compressive strength and toughness values as NC_0PTMC_0 hydrogels, while their elastic modulus values were a factor of 2 lower. A similar observation was reported by others as well. Zhang et al. [15] indicated that PTMC–PEG–PTMC hydrogels with PTMC block lengths higher than 650 g mol^{-1} failed to create robust hydrogels, and Agrawal et al. [28] also showed that in amphiphilic PLA–PEG–PLA hydrogels increasing the length of the hydrophobic PLA block beyond a critical value did not lead to significant enhancement in the elasticity of the gels. Apparently the formation of networks by crosslinking phase-separated micellar dispersion leads to the formation of structures in which the heterogeneity leads to reduced toughness values.

Fig. 2 also shows the effect of the addition of Laponite nanoclay on the mechanical properties of hydrogels. It is clear that the compression modulus of the nanocomposite hydrogels increases with increasing concentrations of Laponite nanoclay, indicating the presence of physical interactions between the Laponite nanoclay platelets and the polymer network chains (Scheme 1). With the addition of 2.5 and 5 wt.% Laponite nanoclay to the crosslinking solution, the elasticity modulus significantly increased. This is especially evident for NC_0TMC_0 hydrogels where the values increased from 15.1 kPa to 47.7 and 66.8 kPa, respectively. For network compositions that contained PTMC, the effect of Laponite nanoclay addition was somewhat less, and was most pronounced when the amount of nanoclay was increased from 2.5 to 5 wt.%. Nevertheless, when compared to non-reinforced hydrogel, these gels were tougher with strain at break values of 81% for $NC_{2.5}PTMC_0$ gels to 96% for NC_5PTMC_1 gels. This suggests that the interactions of the Laponite nanoclay platelets with the PEG component of the hydrogels are stronger than the interactions with the PTMC segments in the networks. Similar trends were also observed for the compressive strengths of the composite hydrogels. As mentioned before, PEG chains readily adsorb to the surface of the hydrophilic Laponite [11,29] and in aqueous micellar block copolymeric systems the hydrophobic PTMC or PLA cores are not able to adsorb to the surfaces of the nanoclay platelets [30].

While in general hydrogels possess advantageous chemical and biological properties, they are usually very brittle and fragile. Importantly, the toughness of the nanocomposite hydrogels was greatly increased with increasing Laponite nanoclay content. Here, too, the enhanced mechanical properties can be attributed to the presence of the nanoclay platelets and the physical interaction of these platelets with the polymer chain segments in the networks (Scheme 1), resulting in arrest of crack propagation. In particular, the high toughness of nanocomposite hydrogels containing 5 wt.% Laponite in the crosslinked solution is significant. The toughest hydrogels were those prepared from macromonomers that did not contain PTMC, i.e. the $NC_{2.5}PTMC_0$ and NC_5PTMC_0 hydrogels. Although increasing the PTMC content in the hydrogels decreased their toughness, a significant reinforcing effect of the nanoclays in $NC_{2.5}PTMC_1$ and NC_5PTMC_1 was noted.

To prepare tough nanocomposite PTMC–PEG–PTMC hydrogels with the desired mechanical properties and swelling characteristics that are still biodegradable, it will be necessary to consider simultaneously the effects of the ratio of PEG to PTMC block length and the nanoclay content.

3.4. In vitro degradation of PTMC–PEG–PTMC hydrogels and nanoclay hydrogel composites by enzymes and macrophages

The degradation of TMC homopolymers and of PEG-PTMC block copolymers was shown to take place via enzymatic processes [31].

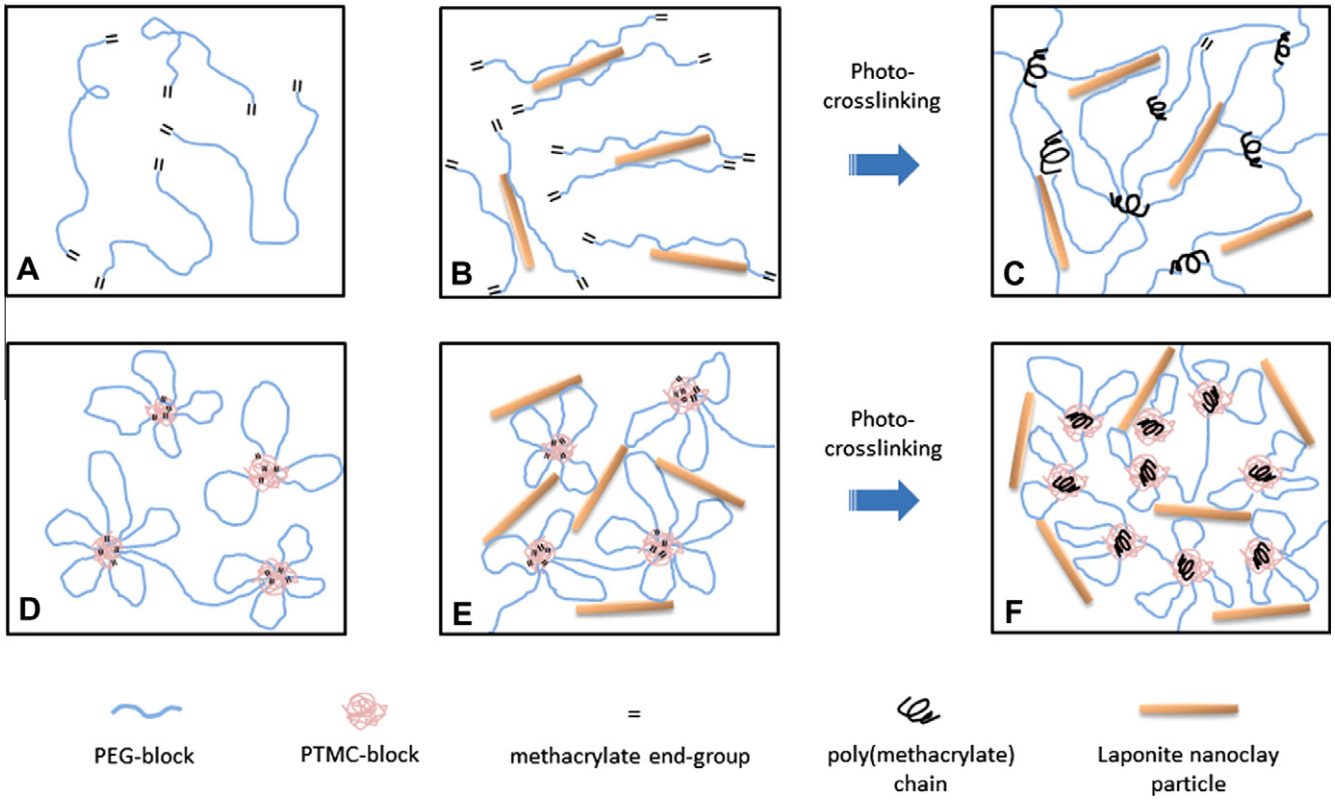

Scheme 1. Schematic diagram of the formation of PEG and PTMC–PEG–PTMC hydrogel networks in the presence of Laponite nanoclay particles. In images (A–C) the formation of a nanocomposite PEG network is illustrated. In (A) an aqueous solution of the MA–PEG–MA macromonomer is illustrated, in the presence of dispersed and exfoliated Laponite nanoclay the PEG segments interact with the nanoclay (B). In (B) the polymerization of the methacrylate end-groups (and concomitant network formation) is illustrated. In images (D–F) the formation of a nanocomposite PTMC–PEG–PTMC network is illustrated. In (D) an aqueous (micellar) dispersion of the MA–PTMC–PEG–PTMC–MA macromonomer is illustrated. These micelles are dynamic in nature, chains can bridge different micelles and a transient network can form. Here, too, the PEG segments of the triblockcopolymeric compound will interact with the nanoclay (E). Note the presence of the methacrylate moieties in the hydrophobic PTMC phase. In (F) the polymerization of the methacrylate end-groups (and concomitant network formation) is illustrated.

To investigate the degradation of the PTMC–PEG–PTMC and their nanoclay composite hydrogels, CE was chosen as the most suitable enzyme.

Fig. 3 shows the loss of mass after incubation in aqueous CE enzyme solutions for 5 weeks. Hydrogels that did not contain TMC were found to be highly stable and resistant to degradation with a loss of less than 5%. When hydrogels were prepared from macromonomers that did contain TMC, enzymatic degradation and mass loss could be observed. The enzyme solutions had become cloudy. After 5 weeks of incubation, the NC_0PTMC_1 and NC_0PTMC_5 hydrogels were almost completely degraded and only small amounts of a gooey mass remained. At this time, $NC_0PTMC_{0.2}$ hydrogels showed a 50% mass loss, while these specimens maintained their shape. The observed increased mass loss for hydrogels containing higher amounts of TMC is in agreement with previous work where the susceptibility of PTMC towards enzymatic degradation in vitro and in vivo was investigated [31].

The incorporation of Laponite nanoclay significantly reduced the extent of degradation of the hydrogels. These reduced degradation rates were most significant for nanocomposite hydrogels containing high amounts of TMC (NC_5PTMC_1 and NC_5PTMC_5). Contrary to the corresponding hydrogels that did not contain nanoclay, these samples preserved their structural integrity during the degradation period. The decreased rates of degradation in the presence of Laponite nanoclay may be the result of a reduced PBS (water) adsorption capacity (see also Fig. 1D) [32,33] and the hindered diffusion of enzymes through the hydrogel matrix [34], resulting from the increased number of physical crosslinkages. The change in affinity of CE towards the PTMC substrate upon adsorption to the Laponite nanocaly surface also needs to be considered [35].

Macrophages play an important role in the in vivo degradation of polymeric materials. We have previously shown in an in vitro model that surface erosion of linear and crosslinked PTMC by these cells can be observed when they are in direct contact with the polymer surface [36]. We now investigated the attachment of macrophages to PEG and PTMC–PEG–PTMC nanocomposite hydrogels and the ensuing degradation and erosion. Screening experiments, where murine macrophages were cultured on TCPS in the presence of the (nanocomposite) hydrogels, showed that the hydrogels did not adversely affect the growth of the cells (data not shown). The macrophages were then cultured on the surface of hydrogels prepared from MA–PEG–MA and MA–$PTMC_1$–PEG–$PTMC_1$–MA macromonomer solutions that contained 0, 2.5 or 5 wt.% Laponite nanoclay.

Fig. 4 shows confocal microscopy images of the macrophages on the surface of the hydrogels after 7 days of culture. Fig. 4A–C show there are not many macrophages on the surface of PEG hydrogels with and without Laponite nanoclay. While other studies have shown that incorporation of nanoclay into non-cell-adhering PEG hydrogels improves the adhesion of cells to the materials [9,37], macrophage adhesion was not significant on our nanocomposite PEG hydrogels.

The incorporation of PTMC in the hydrogels somewhat improved macrophage adhesion to the substrates. By comparing Fig. 4A and D, it can be seen that the number of macrophages present on the surface of NC_0PTMC_1 hydrogels was a little higher than on NC_0PTMC_0 hydrogels. After 10 days of culture the number of macrophages on

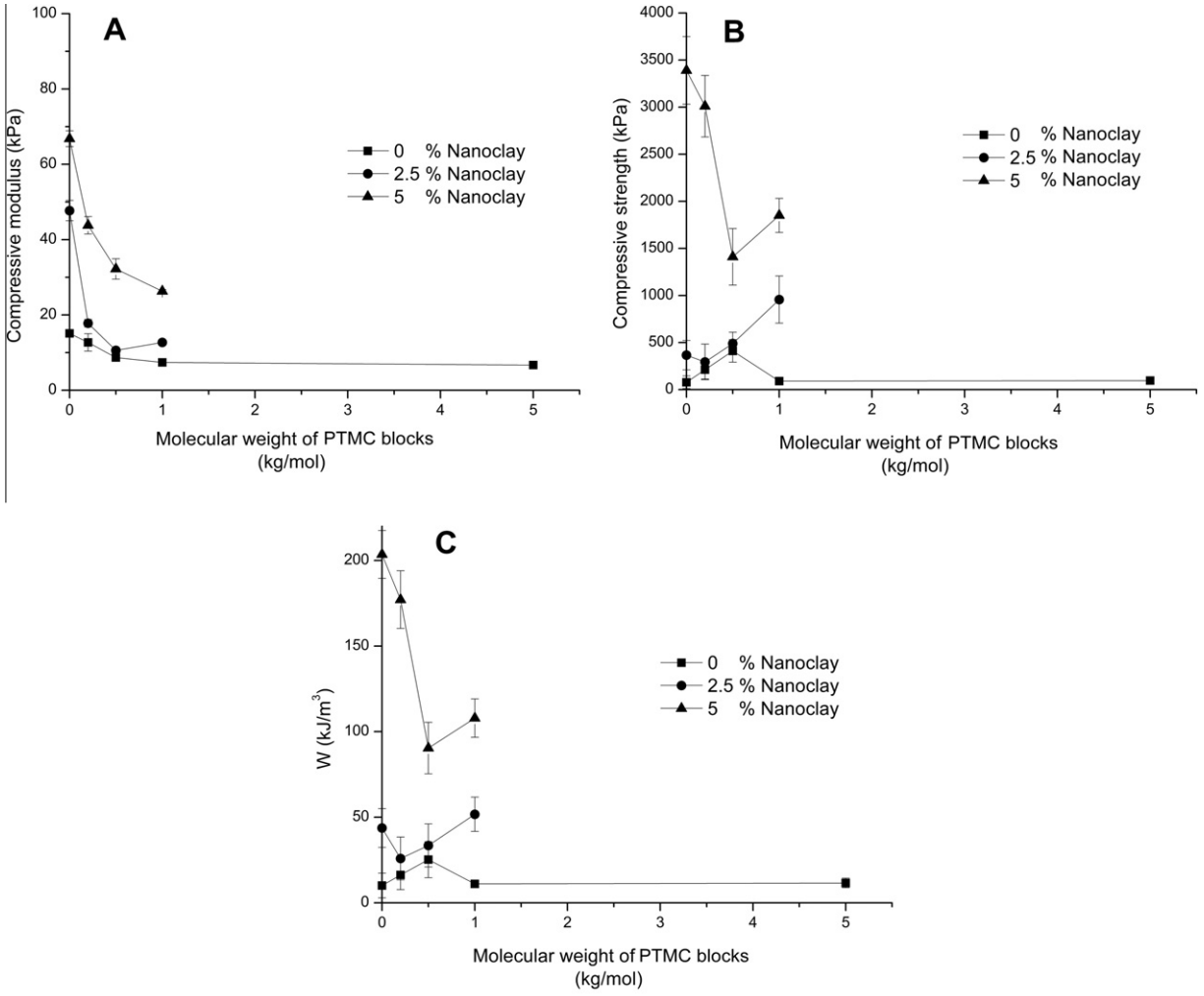

Fig. 2. The effect of the PTMC block length of the PTMC–PEG–PTMC macromonomers and the Laponite XLG nanoclay particle concentration in the crosslinking solution on the mechanical properties of the obtained hydrogels swollen to equilibrium in water: (A) the compressive modulus of the hydrogels; (B) the compressive strength of the hydrogels; (C) the toughness (area under the compressive stress–strain diagram) of the hydrogels.

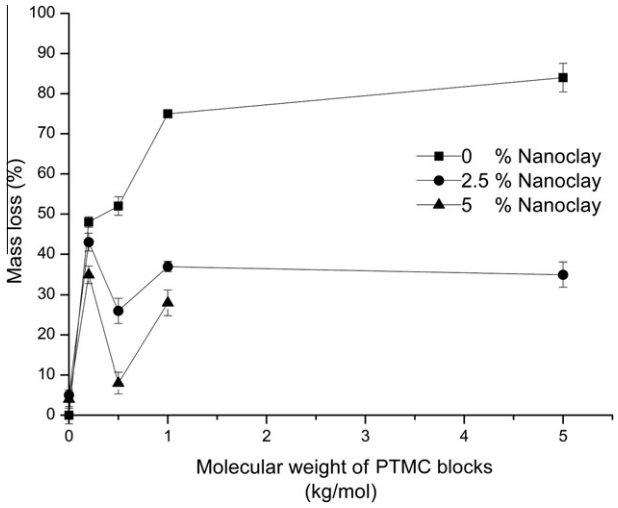

Fig. 3. The effect of the PTMC block length of the PTMC–PEG–PTMC macromonomers and the Laponite XLG nanoclay particle concentration in the crosslinking solution on the enzymatic degradation of the obtained hydrogels after 5 weeks of incubation in an aqueous CE solution.

NC_0PTMC_0 hydrogels had decreased (data not shown) and this difference became even more evident. These results are in agreement with Zhang et al. [15], who showed that hydrophobic PTMC components promote protein adsorption and subsequent cell adhesion.

A highly significant increase in macrophage cell adhesion was observed when Laponite nanoclay particles were incorporated into these PTMC-containing hydrogels (see Fig. 4D–F). At 7 days of culture, the surfaces of $NC_{2.5}PTMC_1$ and of NC_5PTMC_1 hydrogels are completely covered by macrophages. Apparently, this increased hydrophobicity of the nanocomposite hydrogels that results from the increase in PTMC content leads to a synergistic effect and enhanced macrophage attachment [15,37].

Confocal laser scanning microscopy (CLSM) was used to assess the extent of degradation and erosion of the surface of the nanocomposite PEG and PTMC–PEG–PTMC hydrogels. It was indeed observed that the surface of the PEG hydrogels and of the composite PEG hydrogels was not affected by the presence of the few macrophages. However, in addition, the degradation of the surface of NC_0PTMC_1, $NC_{2.5}PTMC_1$ and NC_5PTMC_1 was negligible as the surface of the hydrogels remained unaffected and cells could only be visualized at the surface of the specimens. As also follows from the in vitro enzymatic degradation experiments (see Fig. 3), it could be expected that the composites with the higher Laponite

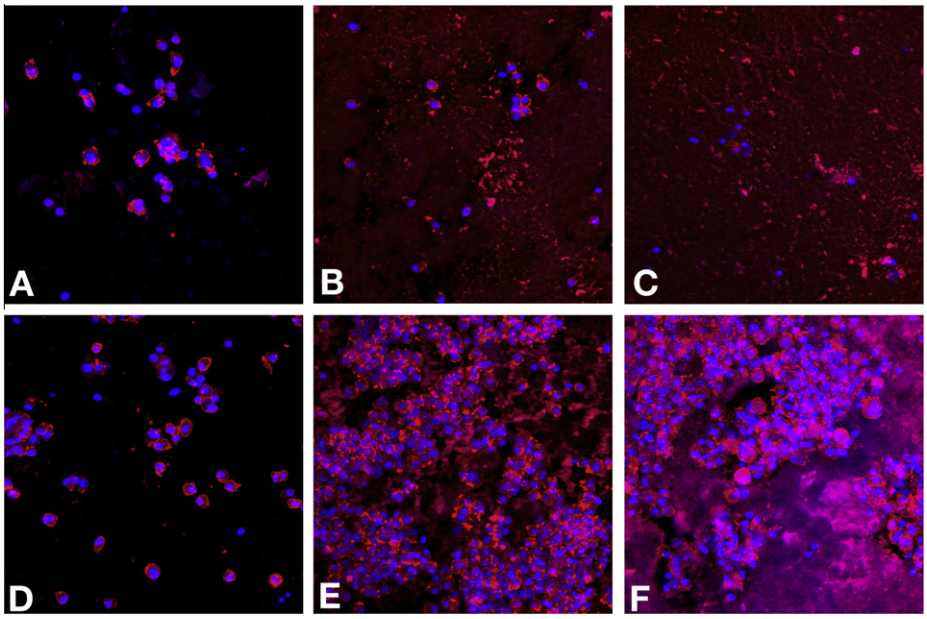

Fig. 4. Confocal laser scanning microscopy images of macrophages adhering to hydrogels prepared from aqueous solutions/dispersions of PEG and PTMC–PEG–PTMC macromonomers and Laponite XLG nanoclay particles after 7 days of cell culturing. The cell nuclei are stained blue, the actin cytoskeleton is stained red. Each image represents an area of 375 μm × 375 μm. PEG nanocomposite hydrogels: (A) NC_0PTMC_0; (B) $NC_{2.5}PTMC_0$; (C) NC_5PTMC_0; PTMC–PEG–PTMC nanocomposite hydrogels: (D) NC_0PTMC_1; (E) $NC_{2.5}PTMC_1$; (F) NC_5PTMC_1.

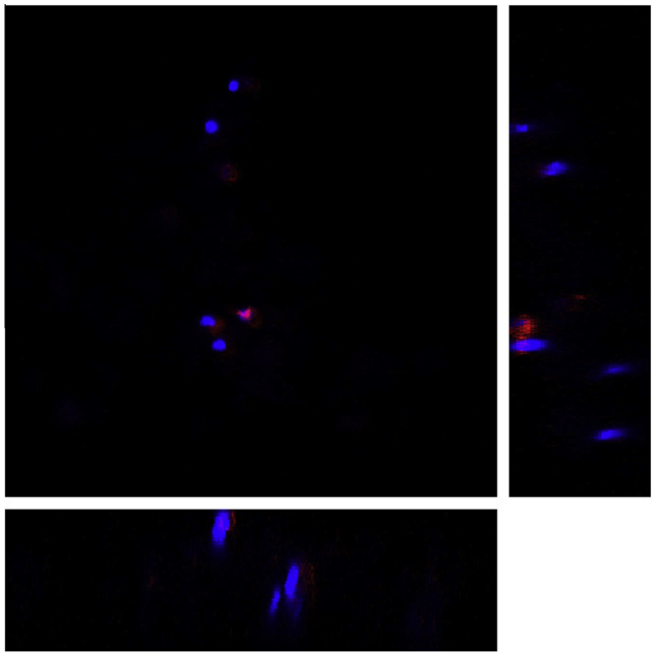

Fig. 5. Confocal laser scanning microscopy image of macrophages adhering to an NC_0PTMC_5 hydrogel that did not contain Laponite XLG nanoclay particles after 10 days of cell culturing. The figure represents one optical section in the image stack, together with cross-sectional labeling profiles along a horizontal and a vertical plane through the stack. The dimensions of the middle image are 375 μm × 375 μm.

nanoclay content would degrade at the lowest rate. Furthermore, because the PTMC block length in the NC_0PTMC_1 network might have been too small to allow enzymatic attack, an additional experiment was conducted in which macrophages were cultured for 7 days on the surface of the hydrogels that contained the longest blocks of PTMC (NC_0PTMC_5) under similar conditions. As Fig. 5 shows, macrophages were able to degrade and erode the surface of the hydrogel. Although in the cross-sections at the right and bottom of Fig. 5 the surface of the nanocomposite hydrogel itself cannot be discerned, the depth of the cells could be seen to vary from 6.5 to 82 μm from the edge of the image.

3.5. Stereolithography

These soft, resilient and tough PTMC–PEG–PTMC hydrogels can be of great interest for use in medical applications such as tissue engineering. With nanocomposite resins containing 15 wt.% MA–$PTMC_{0.5}$–PEG–$PTMC_{0.5}$–MA and 2 wt.% Laponite nanoclay, biodegradable and biocompatible hydrogel structures with a designed architecture of the pore network were prepared by stereolithography. The gyroid pore architecture in the hydrogel that was chosen can facilitate uniform cell distribution within a tissue engineering scaffold upon seeding, attachment and proliferation [38]. The enhanced diffusion and exchange of nutrients and metabolism waste products can lead to higher cell viabilities within the scaffold.

Fig. 6A shows images of the structures that were built by stereolithography after extraction of unreacted macromonomer, dye and the propylene carbonate/water mixture that was used as non-reactive solvent, and swelling in water. By comparing the mass of dried specimens with those of specimens equilibrated in water, very high water absorption of almost 1200% could be determined. The photographs and the microcomputed tomography (μCT) reconstructions (Fig. 6B) clearly indicate that the designed gyroid pore network in the hydrogel structure remains present despite the large extent of swelling in water. Furthermore, the pore network is completely open in the fully hydrated state and will maintain the ability to allow the cells to attach and the flow of medium or body fluids. Characteristic features of the pore network of the built nanocomposite hydrogel structures are presented in Fig. 6C and in Table 2. It is interesting to see that, when comparing the pore size distribution and the average pore size of the water-swollen hydrogel structures determined by μCT with those of the same specimens after drying, the average pore size has increased almost 2-fold and the pore size distribution has shifted to higher pore sizes, while the porosity has decreased significantly upon swelling (Fig. 6D). In these porous

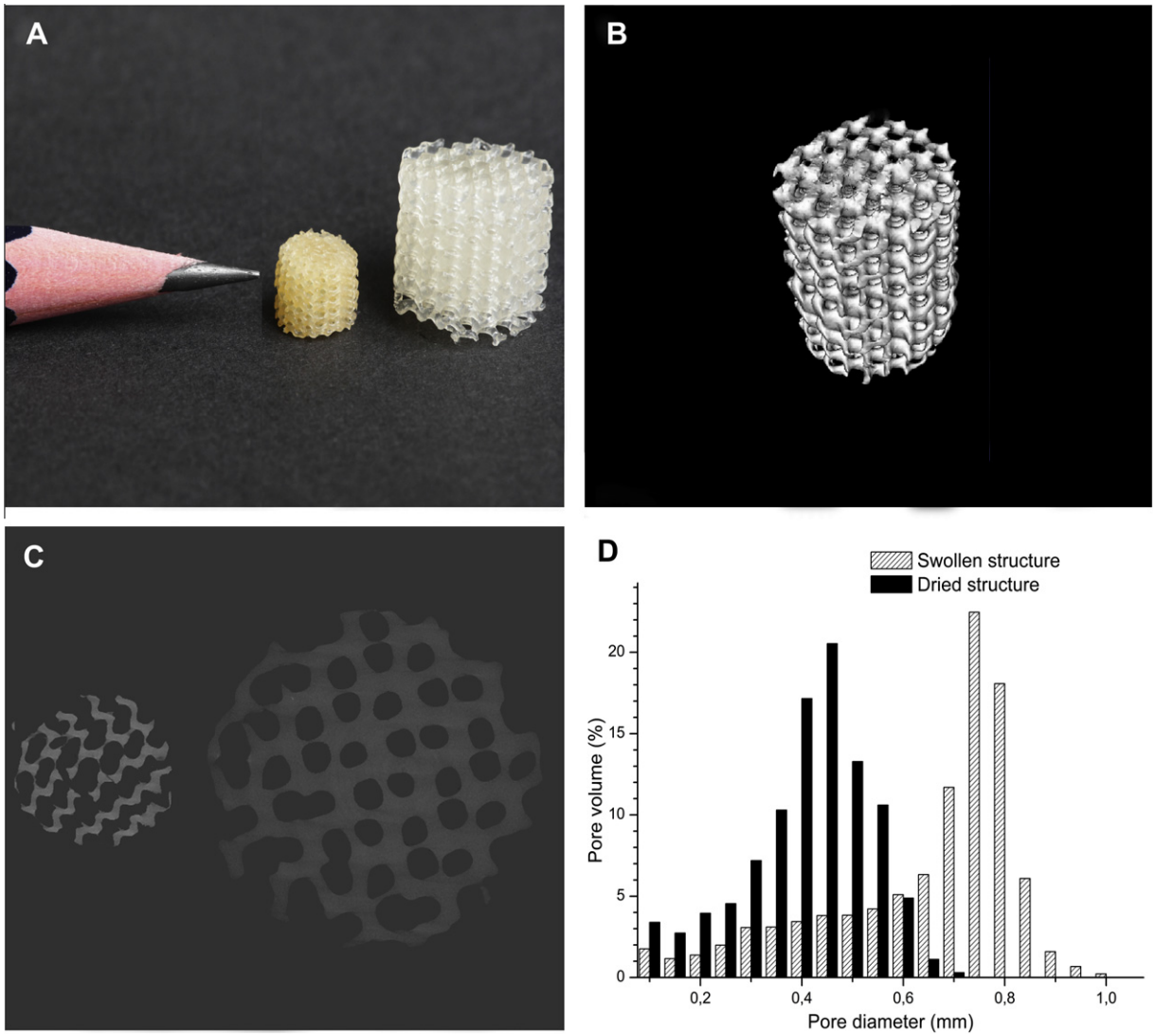

Fig. 6. Designed nanocomposite hydrogel structures prepared by stereolithography using a PTMC–PEG–PTMC macromonomer resin that contained 15 wt.% MA–$PTMC_{0.5}$–PEG–$PTMC_{0.5}$–MA macromer and 2 wt.% Laponite XLG nanoclay particles. (A) Photographic image of built structures with gyroid pore network architecture in the equilibrium water swollen state and after drying. (B) Micro-CT image of the water swollen structures. (C) Micro-CT images of cross-sections taken from the middle parts of the specimens in the equilibrium water-swollen state and after drying. (D) The distribution of the pore sizes of built structures in the equilibrium water-swollen state and after drying.

Table 2
Characteristics of the designed porous structures with gyroid pore network architecture prepared from MA–PTMC–PEG–PTMC–MA macromonomer and Laponite XLG nanoparticle composite resins by stereolithography.

	Diameter (mm)	Height (mm)	Water uptake (%)	Average pore size (μm)	Porosity (%)
Water-swollen structure	11.9 ± 0.8	12.1 ± 0.1	1181 ± 52	750 ± 3	42 ± 2
Dried structure[a]	5.7 ± 0.1	8.1 ± 0.1	–	450 ± 3	65 ± 2

[a] After drying overnight in a vacuum oven at 40 °C.

hydrogels, the final pore size and pore distribution and porosity results from two counteracting effects of the uptake of water: on the one hand, the pore size, and therefore also the porosity, will decrease due to uptake of water in the walls and struts of the structure. On the other hand the specimens as a whole will expand and thereby increase pore size and porosity.

The structures prepared were robust and could be handled with ease, and remained thus in the fully hydrated state. The mechanical properties of these fully hydrated porous hydrogel structures were assessed in compression. The obtained compressive stress–strain diagrams revealed that the structures had a high resistance to fracture, with a maximum compressive stress of 1.12 MPa, a compressive modulus of 33.6 kPa and strain at break of 94%. At strains lower than the strain at break, the structures were able to recover to their original shapes completely upon removal of the compressive stress.

4. Conclusions

Soft biodegradable hydrogels with compression modulus values lower than 100 kPa were prepared by photo-crosslinking aqueous solutions of MA–PTMC–PEG–PTMC–MA containing small amounts of Laponite nanoclay. The compressive strength and toughness of

the resulting hydrogels could be increased by increasing TMC content and more significantly by addition of up 5 wt.% Laponite nanoclay These nanocomposite hydrogels were found to be degraded in vitro by CE and by the action of macrophages adhering to the surface of PTMC–PEG–PTMC nanoclay composite hydrogels.

Using stereolithography, nanocomposite hydrogel structures with a designed gyroid pore network architecture could be prepared from resins that contained MA–PTMC–PEG–PTMC–MA macromonomer and Laponite nanoclay. In the fully hydrated state, these structures had excellent mechanical properties, while the pore network structure could be maintained.

Acknowledgements

We would like to thank Joram Hoekman for his help in the experimental work. This research forms part of the Project P2.01 IDiDAS of the research program of the BioMedical Materials institute, co-funded by the Dutch Ministry of Economic Affairs, Agriculture and Innovation. The financial contribution of the Dutch Arthritis Foundation is gratefully acknowledged.

Appendix A. Figures with essential color discrimination

Certain figures in this article, particularly Figs. 1, 4–6, and Scheme 1, are difficult to interpret in black and white. The full color images can be found in the on-line version, at http://dx.doi.org/10.1016/j.actbio.2012.09.014.

References

[1] Hoffman AS. Hydrogels for biomedical applications. Adv Drug Deliv Rev 2002;54:3–12.
[2] Discher DE, Janmey P, Wang YL. Tissue cells feel and respond to the stiffness of their substrate. Science 2005;310:1139–43.
[3] Engler AJ, Sen S, Sweeney HL, Discher DE. Matrix elasticity directs stem cell lineage specification. Cell 2006;126:677–89.
[4] Calvert P. Hydrogels for soft machines. Adv Mater 2009;21:743–56.
[5] Okumura Y, Ito K. The polyrotaxane gel: a topological gel by figure-of-eight cross-links. Adv Mater 2001;13:485–7.
[6] Haraguchi K, Takehisa T. Nanocomposite hydrogels: a unique organic–inorganic network structure with extraordinary mechanical, optical, and swelling/de-swelling properties. Adv Mater 2002;14:1120–4.
[7] Gong JP, Katsuyama Y, Kurokawa T, Osada Y. Double-network hydrogels with extremely high mechanical strength. Adv Mater 2003;15:1155–8.
[8] Gaharwar AK, Rivera CP, Wu CJ, Schmidt G. Transparent, elastomeric and tough hydrogels from poly(ethylene glycol) and silicate nanoparticles. Acta Biomater 2011;7:4139–48.
[9] Gaharwar AK, Schexnailder PJ, Kline BP, Schmidt G. Assessment of using Laponite (R) cross-linked poly(ethylene oxide) for controlled cell adhesion and mineralization. Acta Biomater 2011;7:568–77.
[10] Li YL, Maciel D, Tomas H, Rodrigues J, Ma H, Shi XY. PH sensitive Laponite/alginate hybrid hydrogels: swelling behaviour and release mechanism. Soft Matter 2011;7:6231–8.
[11] Chang CW, van Spreeuwel A, Zhang C, Varghese S. PEG/clay nanocomposite hydrogel: a mechanically robust tissue engineering scaffold. Soft Matter 2010;6:5157–64.
[12] Gaharwar AK, Kishore V, Rivera C, Bullock W, Wu C-J, Akkus O, et al. Physically crosslinked nanocomposites from silicate-crosslinked PEO: mechanical properties and osteogenic differentiation of human mesenchymal stem cells. Macromol Biosci 2012;12:779–93.
[13] Wang Q, Mynar JL, Yoshida M, Lee E, Lee M, Okuro K, et al. High-water-content mouldable hydrogels by mixing clay and a dendritic molecular binder. Nature 2010;463:339–43.
[14] Wu CJ, Gaharwar AK, Chan BK, Schmidt G. Mechanically tough Pluronic F127/Laponite nanocomposite hydrogels from covalently and physically cross-linked networks. Macromolecules 2011;44:8215–24.
[15] Zhang C, Aung A, Liao LQ, Varghese S. A novel single precursor-based biodegradable hydrogel with enhanced mechanical properties. Soft Matter 2009;5:3831–4.
[16] Zhang C, Sangaj N, Hwang Y, Phadke A, Chang C-W, Varghese S. Oligo(trimethylene carbonate)–poly(ethylene glycol)–oligo(trimethylene carbonate) triblock-based hydrogels for cartilage tissue engineering. Acta Biomater 2011;7:3362–9.
[17] Sharifi S, Kranenburg H-JC, Meij BP, Grijpma DW. Photo-crosslinkable poly(trimethylene carbonate)-based macromers for closure of ruptured intervertebral discs. Macromol Symp 2011;309–310:100–10.
[18] Seck TM, Melchels FPW, Feijen J, Grijpma DW. Designed biodegradable hydrogel structures prepared by stereolithography using poly(ethylene glycol)/poly(D, L-lactide)-based resins. J Control Release 2010;148:34–41.
[19] Pêgo AP, Poot AA, Grijpma DW, Feijen J. Physical properties of high molecular weight 1,3-trimethylene carbonate and D, L-lactide copolymers. J Mater Sci Mater Med 2003;14:767–73.
[20] Nijenhuis AJ, Colstee E, Grijpma DW, Pennings AJ. High molecular weight poly(L-lactide) and poly(ethylene oxide) blends: thermal characterization and physical properties. Polymer 1996;37:5849–57.
[21] Bat E, Grijpma DW, Feijen J. Thermoreversible gelation behaviour of PTMC–PEG–PTMC triblock copolymers. J Control Release 2008;132:e37–9.
[22] Kim BS, Oh JM, Cho JS, Lee SH, Lee B, Khang G, et al. Comparison of micelles formed by amphiphilic poly(ethylene glycol)-b-poly(trimethylene carbonate) star block copolymers. J Appl Polym Sci 2009;111:1706–12.
[23] Ng WK, Tam KC, Jenkins RD. Rheological properties of methacrylic acid/ethyl acrylate co-polymer: comparison between an unmodified and hydrophobically modified system. Polymer 2001;42:249–59.
[24] Hensen EJM, Smit B. Why clays swell. J Phys Chem B 2002;106:12664–7.
[25] Sperling LH. Introduction to physical polymer science. 4th ed. New York: Wiley Interscience; 2006.
[26] Hu X, Wang T, Xiong L, Wang C, Liu X, Tong Z. Preferential adsorption of poly(ethylene glycol) on hectorite clay and effects on poly(*N*-isopropylacryl amide)/hectorite nanocomposite hydrogels. Langmuir 2009;26:4233–8.
[27] Sanabria-DeLong N, Crosby AJ, Tew GN. Photo-cross-linked PLA–PEO–PLA hydrogels from self-assembled physical networks: mechanical properties and influence of assumed constitutive relationships. Biomacromolecules 2008;9:2784–91.
[28] Agrawal SK, Sanabria-DeLong N, Tew GN, Bhatia SR. Rheological characterization of biocompatible associative polymer hydrogels with crystalline and amorphous endblocks. J Mater Res 2006;21:2118–25.
[29] Nelson A, Cosgrove T. A small-angle neutron scattering study of adsorbed poly(ethylene oxide) on Laponite. Langmuir 2004;20:2298–304.
[30] Agrawal SK, Sanabria-DeLong N, Tew GN, Bhatia SR. Nanoparticle-reinforced associative network hydrogels. Langmuir 2008;24:13148–54.
[31] Zhang Z, Kuijer R, Bulstra SK, Grijpma DW, Feijen J. The in vivo and in vitro degradation behavior of poly(trimethylene carbonate). Biomaterials 2006;27:1741–8.
[32] Martucci JF, Ruseckaite RA. Biodegradation of three-layer laminate films based on gelatin under indoor soil conditions. Polym Degrad Stabil 2009;94:1307–13.
[33] Spiridon I, Popescu MC, Bodarlau R, Vasile C. Enzymatic degradation of some nanocomposites of poly(vinyl alcohol) with starch. Polym Degrad Stabil 2008;93:1884–90.
[34] Zhuang H, Zheng JP, Gao H, Yao KD. In vitro biodegradation and biocompatibility of gelatin/montmorillonite-chitosan intercalated nanocomposite. J Mater Sci Mater M 2007;18:951–7.
[35] Serefoglou E, Litina K, Gournis D, Kalogeris E, Tzialla AA, Pavlidis IV, et al. Smectite clays as solid supports for immobilization of beta-glucosidase: synthesis, characterization, and biochemical properties. Chem Mater 2008;20:4106–15.
[36] Bat E, van Kooten TG, Feijen J, Grijpma DW. Macrophage-mediated erosion of gamma irradiated poly(trimethylene carbonate) films. Biomaterials 2009;30:3652–61.
[37] Schexnailder PJ, Gaharwar AK, Bartlett II RL, Seal BL, Schmidt G. Tuning cell adhesion by incorporation of charged silicate nanoparticles as cross-linkers to polyethylene oxide. Macromol Biosci 2010;10:1416–23.
[38] Olivares AL, Marshal E, Planell JA, Lacroix D. Finite element study of scaffold architecture design and culture conditions for tissue engineering. Biomaterials 2009;30:6142–9.